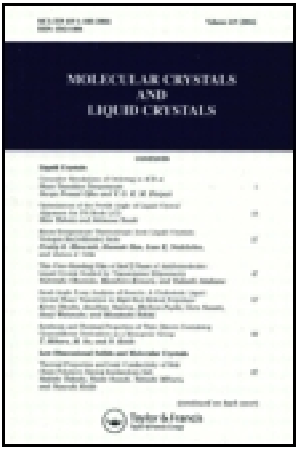

Molecular Crystals and Liquid Crystals

P-I-N Junction Organic Solar Cells

Masahiro Hiramoto [a] , Kouji Suemori [a] , Yoshio Matsumura [a] , Takahiro Miyata [a] & Masaaki Yokoyama [a]

[a] Material and Life Science, Graduate School of Engineering, Osaka University, Yamadaoka, Suita, Osaka, Japan

To cite this article: Masahiro Hiramoto, Kouji Suemori, Yoshio Matsumura, Takahiro Miyata & Masaaki Yokoyama (2006): P-I-N Junction Organic Solar Cells, Molecular Crystals and Liquid Crystals, 455:1, 267-275

To link to this article: http://dx.doi.org/10.1080/15421400600698683

Mol. Cryst. Liq. Cryst., Vol. 455, pp. 267–275, 2006
Copyright © Taylor & Francis Group, LLC
ISSN: 1542-1406 print/1563-5287 online
DOI: 10.1080/15421400600698683

P-I-N Junction Organic Solar Cells

Masahiro Hiramoto
Kouji Suemori
Yoshio Matsumura
Takahiro Miyata
Masaaki Yokoyama
Material and Life Science, Graduate School of Engineering, Osaka University, Yamadaoka, Suita, Osaka, Japan

10 cm^2 area molecular photovoltaic cells have been fabricated, incorporating transparent protection layers of naphthalene tetracarboxylic anhydride (NTCDA), completely suppressing electrical shorting. Even a 2 μm-thick NTCDA layer was unable to degrade cell performance. Three-layered organic solar cells incorporating a codeposited interlayer of fullerene and metal-free phthalocyanine, whose nanostructure was optimized by controlling the substrate temperature during coevaporation, showed a photoelectric conversion efficiency of 2.5% under illumination with simulated solar light. The three-layered cells were concluded to have a p-i-n energetic structure.

Keywords: codeposited interlayer; large area cells; organic solar cells; p-i-n energetic structure; thick transparent protection layer

INTRODUCTION

Organic solar cells, consisting of vacuum-deposited molecular thin films have been intensively studied, following the *p-n* heterojunction cells reported by Tang [1–3]. However, most researchers have been forced to fabricate very small cells of the order of only millimeters in size. Since the photocarrier generation occurs only at the heteromolecular interface in the *p-n* heterojunction cell, cell thickness should be less than 100 nm to optimize the cell performance [1,4,5]. Unfortunately, the electrical shorting, caused by the metal migration along

Address correspondence to Masahiro Hiramoto, Material and Life Science, Graduate School of Engineering, Osaka University, Yamadaoka, Suita, Osaka, 565-0871, Japan. E-mail: hiramoto@chem.eng.osaka-u.ac.jp

grain boundaries, to a depth of more than 100 nm into the film, frequently occurred during the vacuum-deposition of counter electrodes. This is a weak point when compared to polymer cells, of which large area cells have been fabricated [2,3,6]. Recently, we found, by chance, that the insertion of transparent naphthalene tetracarboxylic anhydride (NTCDA, Fig. 1) films under vacuum-deposited metal electrodes effectively protected cells from shorting-out electrically [4]. Thus, we decided to fabricate large area cells, utilizing these NTCDA protection layers. As an organic *p*-*n* heterojunction, we adopted a combination of metal-free phthalocyanine (H_2Pc) and fullerene (C_{60}) [7].

On the other hand, mixed films of two kinds of organic semiconductors that act as donors and acceptors possess high potential for photocarrier generation [2,3]. We previously reported *p*-*i*-*n* organic solar cells in which the *i* interlayer is a codeposited film of organic semiconductors [8,9]. Since the nanostructure of codeposited films is obviously believed to influence the photocurrent generation process, we have tried to control the nanostructure of codeposited films by varying the substrate temperature during vacuum coevaporation [10]. Thus, we decided to control the nanostructure of C_{60}:H_2Pc codeposited films and to incorporate them into *p*-*i*-*n* type cells.

Here, we report on 10 cm^2 area *p*-*n* heterojunction cells, protected by a 2 μm-thick NTCDA layer, and the three-layered organic solar cells incorporating a nanostructure-controlled C_{60}:Pc codeposited interlayer. A photoelectric conversion efficiency of 2.5% was observed.

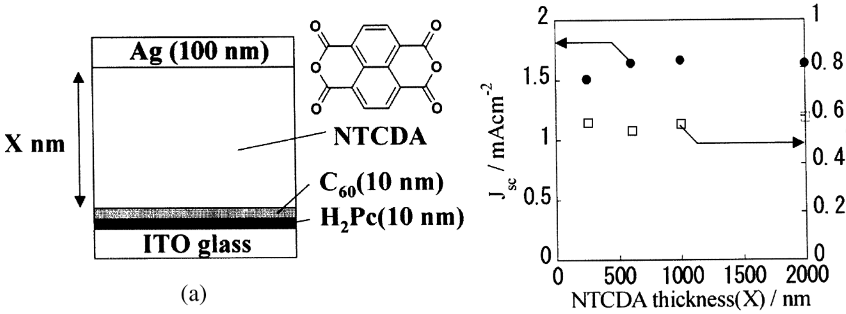

(a)

(b)

FIGURE 1 (a) Cell structure and chemical formula of NTCDA. (b) Dependence of J_{sc} and FF on the NTCDA thickness (X). Cell area was 0.4 cm × 0.05 cm (0.02 cm^2). Cells were illuminated with simulated solar light (AM1.5, 100 mWcm^{-2}) at an ambient pressure of 0.1 Pa.

EXPERIMENTAL

C_{60}, metal-free phthalocyanine (H_2Pc), naphthalene tetracarboxylic anhydride (NTCDA) and Ag counter electrodes were deposited by the vacuum evaporation technique under 1×10^{-3} Pa onto indium tin oxide (ITO) glass substrates. Codeposition was performed by coevaporation from two separately controlled sources. The substrate temperature was controlled using a substrate heater (ULVAC Kiko, Inc.). The photovoltaic properties were measured under irradiation with simulated solar light (Yamashita Denso, Co., Ltd., YSS-50A). All of the measurements were performed at room temperature under vacuum conditions (10^{-1} Pa).

RESULTS AND DISCUSSION

Large Area Organic Solar Cells with Thick Protection Layers

Figure 1(a) and (b) show the cell structure and the dependence of short-circuit photocurrent (J_{sc}) and fill factor (FF) on NTCDA thickness (X). Surprisingly, even though 2 μm-thick NTCDA was inserted between the Ag electrode and the H_2Pc/C_{60} layer, degradation of either parameters was hardly observed. In particular, the absence of FF degradation means that there was no influence of bulk resistance on the carrier transport in the NTCDA film. ITO/C_{60} (10 nm)/H_2Pc (10 nm)/Ag cells could not be fabricated due to electrical shorting. Above X = 250 nm, electrical shorting-out was completely suppressed. Figure 2 shows a scanning electron microscopic (SEM) image of the cross section of a 2 μm-thick NTCDA film. The NTCDA film possesses a columnar structure and there are few grain boundaries directed towards the electrodes. Thus, electrons, photogenerated at the C_{60}/H_2Pc heterojunction, transport readily through the NTCDA. It should be noted that, when thick C_{60} films were used instead of NTCDA to prevent shorting-out, serious suppression of J_{sc} and FF were observed and it was confirmed that the many grain boundaries existed in C_{60} film.

By using cells with 2 μm-thick NTCDA protection layers, we endeavored to increase the cell area in turn to 0.05 cm × 0.4 cm (0.02 cm^2) (Fig. 3(a), left), 0.75 cm × 0.75 cm (0.56 cm^2), 1 cm × 1 cm (1 cm^2), 3.2 cm × 3.2 cm (10.24 cm^2) (Fig. 3(a), right), and 5 cm × 5 cm (25 cm^2). All cells, other than 25 cm^2, could be fabricated without electrical shorting. In the case of the 25 cm^2 device, we confirmed that the electrical short was caused by one or two dust particles on the substrate. Figure 3(b) shows the current-voltage characteristics of a 10 cm^2 cell (solid curve). This cell was able to produce a photocurrent of 15 mA

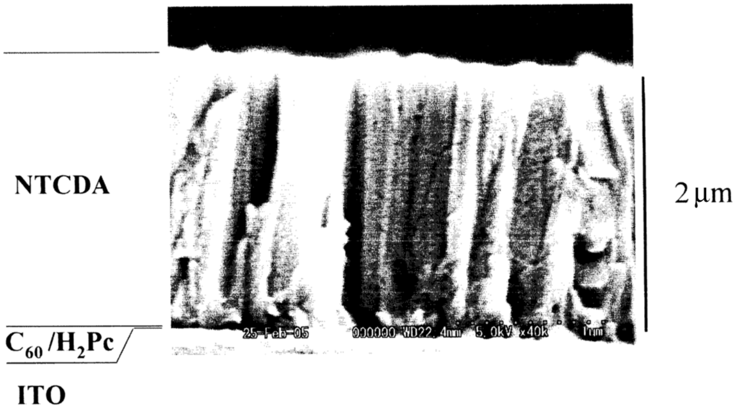

FIGURE 2 SEM image of cross section of a cell incorporating a 2 µm-thick NTCDA protection layer.

under short-circuit conditions (left vertical axis). On the other hand, the photocurrent density (right vertical axis) was almost the same for the 10 cm^2 (solid curve) and 0.02 cm^2 cells (dotted curve). This implies that the magnitude of photocurrent is proportional to the cell area. The FF decrease in the 10 cm^2 cell can be attributed to the increase in the resistance of ITO electrode with increasing cell area.

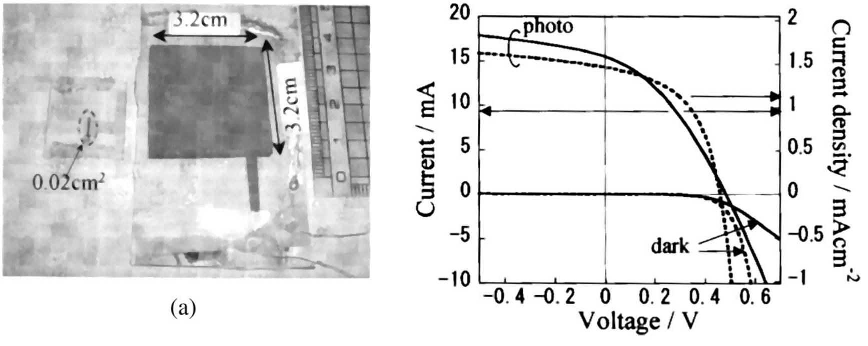

(a)

(b)

FIGURE 3 (a) Photograph of the cells with an area of 0.02 (left) and 10 cm^2 (right). (b) Current (left vertical axis), current density (right vertical axis)–voltage characteristics for cells with areas of 10 cm^2 (solid curve) and 0.02 cm^2 (dotted curve). Cell structure comprised ITO/H_2Pc (10 nm)/C_{60} (10 nm)/NTCDA (2 µm)/Ag (100 nm). Simulated solar light (AM1.5, 100 mWcm^{-2}) was irradiated at an ambient pressure of 0.1 Pa.

Thus, in order to increase cell area further, the lateral resistance of the ITO electrode should be reduced by incorporating comb-type metal electrodes.

P-I-N Junction Organic Solar Cells Incorporating a Nanostructure Optimized H_2Pc:C_{60} Codeposited Interlayer

We have optimized the substrate temperature for the photovoltaic performance of the single-layered cells of C_{60}:H_2Pc codeposited film. Pronounced enhancement of the magnitude of the short-circuit photocurrent density (J_{sc}) was observed by heating to around +80°C [11].

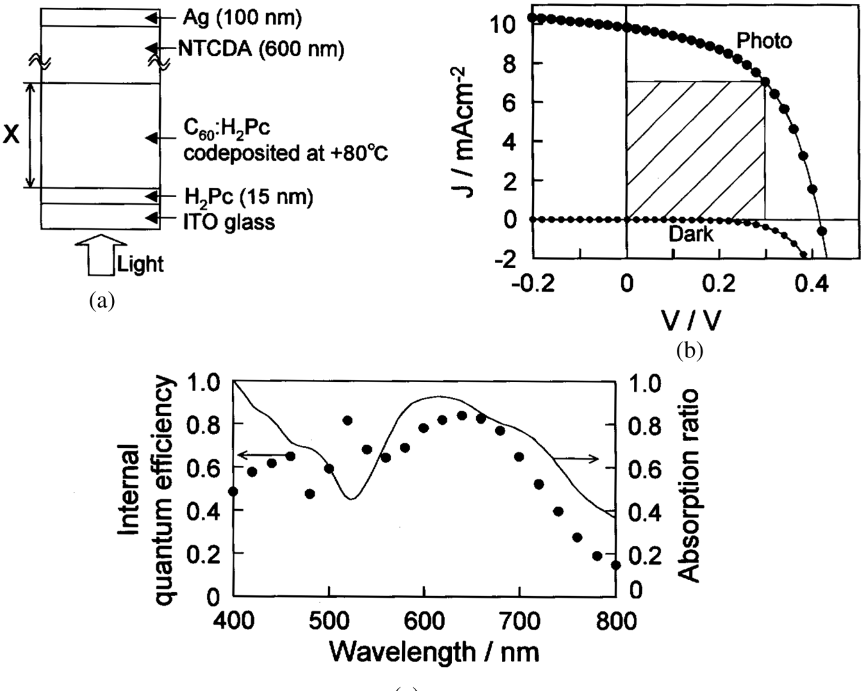

(a)

(b)

(c)

FIGURE 4 (a) Three-layered cell. (b) Current-voltage (J-V) characteristics of a three-layered cell incorporating a 130-nm-thick C_{60}:H_2Pc (5:6) interlayer co-deposited at +80°C. Performance; J_{sc}: 9.9 $mAcm^{-2}$, V_{oc}: 0.42 V, FF: 0.52, Efficiency: 2.5%. The intensity of simulated solar light transmitted through the ITO glass substrate was 85.8 $mWcm^{-2}$. (c) Spectral dependence of internal quantum efficiency of J_{sc} (closed dots) and absorption ratio of incident light by organic film (solid curve).

Thus, we decided to incorporate a C_{60}:H_2Pc layer deposited at +80°C into a three-layered cell (Fig. 4(a)). The co-deposited layer was sandwiched between *n*-type NTCDA and *p*-type H_2Pc. Very thick NTCDA layer (600 nm) was used to avoid the electrical shorting-out of the cells. The best photovoltaic performance [J_{sc}: 9.9 mAcm^{-2}, V_{oc}: 0.42 V, FF: 0.52, photo-electric conversion efficiency: 2.5%] was observed when the thickness and the C_{60}:H_2Pc ratio of the co-deposited layer were optimized to 130 nm and 5:6, respectively (Fig. 4(b)). Figure 4(c) shows the spectral dependence of the internal quantum efficiency of J_{sc} (closed dots) and the absorption ratio of the incident light absorbed by the organic film (solid curve). The quantum efficiency is calculated as the ratio of the number of carriers collected under short-circuit conditions to the number of photons absorbed by the organic layers. The maximum and the averaged internal quantum efficiencies (400 nm–800 nm) were 84% and 59.3%, respectively. From the solid curve, the total absorption ratio and the intensity absorbed

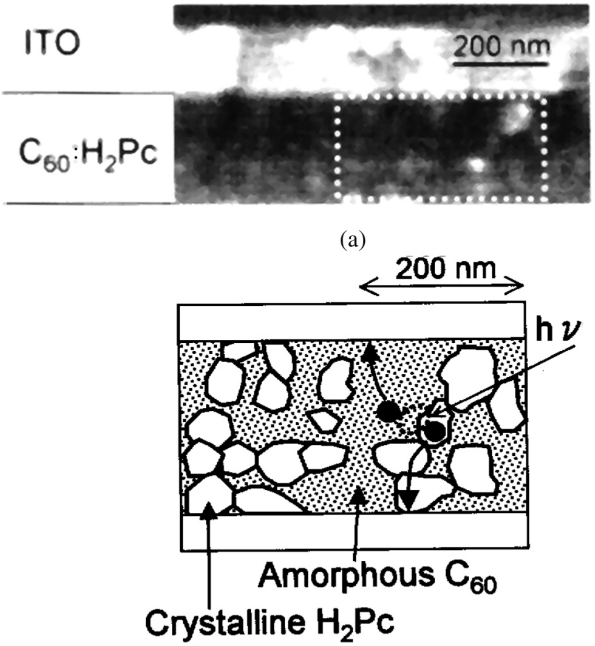

(a)

(b)

FIGURE 5 (a) SEM image of a cross section of a C_{60}:H_2Pc film fabricated on a substrate heated at +80°C. (b) Morphological illustration of a cross section, drawn by tracing the image within the dotted box in Figure 5(a).

by the organic layer for simulated solar light can be calculated as 53% (300 nm–1100 nm) and 45.5 mWcm^{-2}, respectively. Thus, the conversion efficiency with respect to absorbed solar light is calculated as 4.7%. Both the internal quantum efficiency and the absorption ratio (utilization efficiency of solar light) can stand further improvements.

Figure 5(a) shows an image of a cross section of a C_{60}:H_2Pc film codeposited at +80°C observed using a scanning electron microscope (SEM). A lot of nanocrystals of approximately 50 nm in diameter that were surrounded by a smooth region were observed. X-ray diffraction (XRD) identified that the nanocrystals consisted of H_2Pc, since a clear XRD peak that was characteristic of H_2Pc ($2\theta = 7°$) was observed. In Figure 5(b), a morphological illustration of the cross section is depicted. The film has a nanocomposite structure somewhere between crystalline H_2Pc and amorphous C_{60}. We concluded that efficient photocurrent generation is due to the formation of spatially-separated

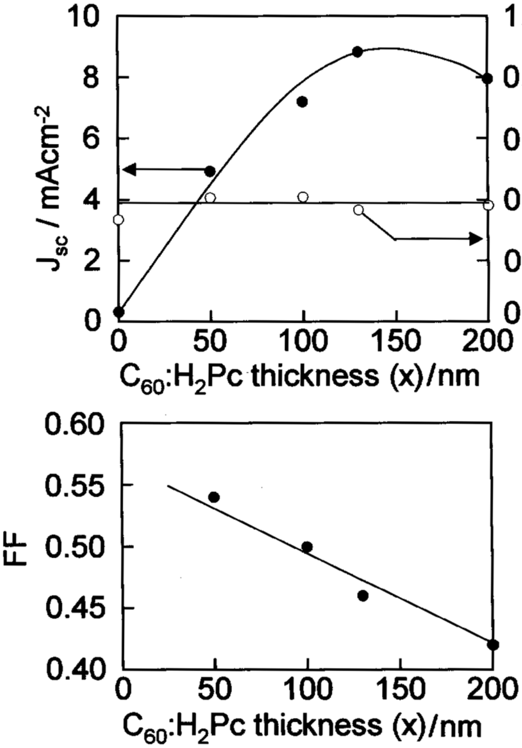

FIGURE 6 Dependence of J_{sc}, V_{oc} and FF of the three-layered cells on C_{60}:H_2Pc thickness (x). C_{60}:H_2Pc ratio was 1:1.

routes for electrons and holes. Thus, the entire bulk of the thick C_{60}:H_2Pc film could contribute to photocurrent generation.

Figure 6 shows the dependence of J_{sc}, V_{oc} and FF of the three-layered cells (Fig. 4(a)) on the thickness (x) of the C_{60}:H_2Pc. J_{sc} increased with increasing x up to 130 nm and then started to decrease. V_{oc} showed a constant value of approximately 0.4 V. FF decreased monotonically with increasing x. These characteristics can be reasonably explained based on a *p-i-n* energetic structure (Fig. 7). The V_{oc} value of 0.4 V corresponds well with the built-in potential (0.4 eV) estimated by the Kelvin vibrating capacitor method [12]. Even without C_{60}:H_2Pc layer ($x = 0$ nm), i.e., Ag/NTCDA/H_2Pc/ITO cell, almost the same value of V_{oc} was observed. Thus, we concluded that a built-in electric field, created by the difference in the Fermi levels (E_F) of NTCDA and H_2Pc, is distributed across the C_{60}:H_2Pc interlayer and drives efficient charge-carrier generation and charge transport in the co-deposited layer. The increase in J_{sc} between $x = 0$ nm and 130 nm is due to the increase in the absorption ratio of solar light

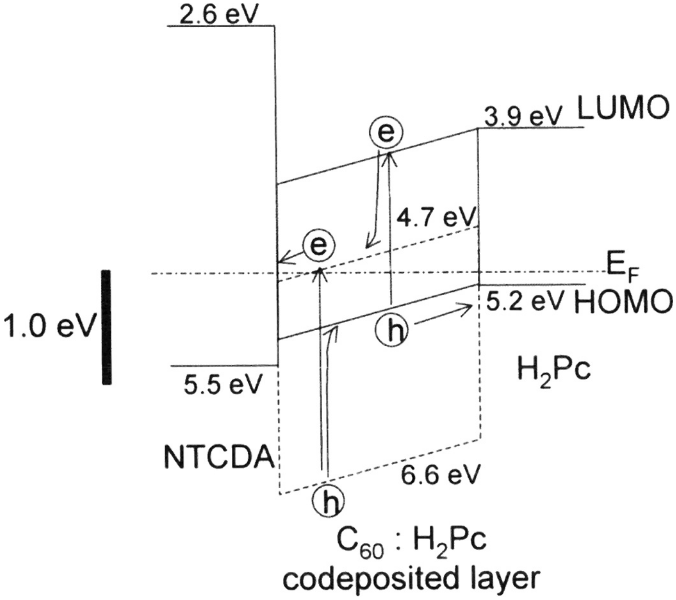

FIGURE 7 *p-i-n* energetic structure of the three-layered cell. The energetic relationships are precisely illustrated with respect to the scale bar. The C_{60} in the co-deposited layer is depicted using a broken line. Numerical values are energetic positions of levels for respective H_2Pc, C_{60}, and NTCDA films before forming junction.

induced by the C_{60}:H_2Pc interlayer. The decrease in J_{sc} above $x = 130\,nm$ is due to an increase in the resistance of the co-deposited layer with increasing x, which also causes a monotonic decrease in FF. Those observations support the *p-i-n* energetic structure.

CONCLUSION

The operation of molecular photovoltaic cells with an area of $10\,cm^2$ were successfully demonstrated. Cells incorporating thick NTCDA films appeared to be free from the influence of bulk resistance. *p-i-n* junction organic solar cells incorporating an amorphous C_{60}:crystalline H_2Pc nanocomposite interlayer showed photo-electric conversion efficiencies of 2.5%.

REFERENCES

[1] Tang, C. W. (1986). *Appl. Phys. Lett.*, *48*, 183.

[2] Sun, S.-S. & Sariciftci, N. S. (Eds.) (March, 2005). *Organic Photovoltaics, Mechanisms, Materials and Devices*, CRC Press: New York.

[3] Spanggaard, H. & Krebs, F. C. (2004). *Sol. Energy Mater. Sol. Cells*, *83*, 125, and references therein.

[4] Suemori, K., Miyata, T., Yokoyama, M., & Hiramoto, M. (2004). *Appl. Phys. Lett.*, *85*, 6269.

[5] Peumans, P., Bulovic, V., & Forrest, S. R. (2000). *Appl. Phys. Lett.*, *76*, 2650.

[6] Shaheen, S. E., Brabec, C. J., Sariciftci, N. S., Padinger, F., Fromherz, T., & Hummelen, J. C. (2001). *Appl. Phys. Lett.*, *78*, 841.

[7] Rostalski, J. & Meissner, D. (2000). *Solar Energy Materials and Solar Cells*, *61*, 87.

[8] Hiramoto, M., Fujiwara, H., & Yokoyama, M. (1991). *Appl. Phys. Lett.*, *58*, 1062.

[9] Hiramoto, M., Fujiwara, H., & Yokoyama, M. (1992). *J. Appl. Phys.*, *72*, 3781.

[10] Hiramoto, M., Suemori, K., & Yokoyama, M. (2002). *Jpn. J. Appl. Phys.*, *41*, 2763.

[11] Suemori, K., Miyata, T., Hiramoto, M., & Yokoyama, M. (2004). *Jpn. J. Appl. Phys.*, *43*, L1014.

[12] Saito, S., Soumura, T., & Maeda, T. (1984). *J. Vac. Sci. Technol.*, *A2*, 1389.